# BRL

MEMORANDUM REPORT NO. 2546

# PARAMETRIC SENSITIVITY STUDY OF A NUMERICAL MODEL FOR FLAME SPREADING





Clarence W. Kitchens, Jr.

October 1975



USA BALLISTIC RESEARCH LABORATORIES
ABERDEEN PROVING GROUND, MARYLAND

Destroy this report when it is no longer needed.
Do not return it to the originator.

Secondary distribution of this report by originating or sponsoring activity is prohibited.

Additional copies of this report may be obtained from the National Technical Information Service, U.S. Department of Commerce, Springfield, Virginia 22151.

The findings in this report are not to be construed as an official Department of the Army position, unless so designated by other authorized documents.

UNCLASSIFIED

SECURITY CLASSIFICATION OF THIS PAGE (When Data Entered)

## REPORT DOCUMENTATION PAGE

READ INSTRUCTIONS BEFORE COMPLETING FORM

1. REPORT NUMBER: MEMORANDUM REPORT NO. 2546
2. GOVT ACCESSION NO.
3. RECIPIENT'S CATALOG NUMBER

(6) 4. TITLE (and Subtitle): Parametric Sensitivity Study of a Numerical Model for Flame Spreading.

(9) 5. TYPE OF REPORT & PERIOD COVERED: FINAL report.

6. PERFORMING ORG. REPORT NUMBER

(10) 7. AUTHOR(s): Clarence W. Kitchens, Jr

8. CONTRACT OR GRANT NUMBER(s): RDT&E 1T161102A336; RDT&E 1T161102A32C

9. PERFORMING ORGANIZATION NAME AND ADDRESS: USA Ballistic Research Laboratories, Aberdeen Proving Ground, Maryland 21005

10. PROGRAM ELEMENT, PROJECT, TASK AREA & WORK UNIT NUMBERS

11. CONTROLLING OFFICE NAME AND ADDRESS: US Army Materiel Command, 5001 Eisenhower Avenue, Alexandria, VA 22333

(11) 12. REPORT DATE: OCT 75

13. NUMBER OF PAGES: 33

14. MONITORING AGENCY NAME & ADDRESS (if different from Controlling Office)

(12) 31p.

15. SECURITY CLASS. (of this report): UNCLASSIFIED

15a. DECLASSIFICATION/DOWNGRADING SCHEDULE

16. DISTRIBUTION STATEMENT (of this Report)

Approved for public release; distribution unlimited.

(14) BRL-MR-2546

17. DISTRIBUTION STATEMENT (of the abstract entered in Block 20, if different from Report)

(16) RDT/E-1-T-161102-A-336,

18. SUPPLEMENTARY NOTES: RDT/E-1-T-161102-A-32-C

19. KEY WORDS (Continue on reverse side if necessary and identify by block number)

| | | |
|---|---|---|
| Flame Spreading | Dynamic Burning Rate | Heat Transfer |
| Ignition | Method of Characteristics | Drag |
| Sensitivity | Compressible Flow | Particle Size |
| Numerical Solution | Porosity | Fluid Dynamics |

20. ABSTRACT (Continue on reverse side if necessary and identify by block number)

(jpl)

A sensitivity study is performed to identify critical input assumptions in a numerical model for flame spreading. This model is applied to predict flame spreading phenomena in a bed of small arms ball propellant. The numerical results are compared with experimental pressure measurements taken in 5.85 and 10.84 cm long venting chambers. The predicted flame spreading rate is approximately three times slower than is indicated in the experiments. The sensitivity calculations identify the relative importance of assumptions about

Next page

DD FORM 1 JAN 73 1473 EDITION OF 1 NOV 65 IS OBSOLETE

050 750

UNCLASSIFIED

SECURITY CLASSIFICATION OF THIS PAGE (When Data Entered)

the average particle size, ignition criteria, drag correlation, heat transfer correlation, compaction distance, porosity distribution, and burning rate. The compaction distance and initial porosity distribution are identified as important parameters in this model. It appears that a two-phasc flow model is required for more realistic flame spreading simulations.

TABLE OF CONTENTS

LIST OF ILLUSTRATIONS

# I. INTRODUCTION

The classical treatment of gun interior ballistics neglects the description of flame spreading and assumes that the propellant charge is initially fully ignited. This assumption is usually justified for charges with efficient igniter systems since the flame spreading interval is very short; e.g., several milliseconds or less. The flame spreading interval can become very important in some charges due to poor design and/or malfunction of the igniter system. Ignition waves can result from localized ignition of the propellant charge and the subsequent flame spreading into the unignited propellant.

A model describing the passage of a gas pressure wave and flame front through a stationary packed bed of ball propellant has been developed by Kuo et al[1]. Numerical results were obtained by Kuo using a finite-difference technique to demonstrate the validity of the model. A method of characteristics computer program using an alternate method for solving these same governing equations has been developed by Kitchens[2]. This program has been used to study gas flow and pressure transients during flame spreading[2,3]. The characteristics solutions presented in Reference 2 are in general agreement with the finite-difference results of Reference 1. Both numerical methods predict the trends of experimental pressure-time measurements taken in a 3.81 cm long venting chamber, although the results differ in detail.

Comparisons of the numerical solutions obtained by this characteristics program with experimental pressure measurements in longer chambers have shown that the present model does not account for some of the phenomena observed experimentally. This report describes a series of numerical parametric sensitivity studies that have been carried out with the characteristics program to help identify the important input

---

1. *K. K. Kuo, R. Vichnevetsky and M. Summerfield, "Theory of Flame Front Propagation in Porous Propellant Charges Under Confinement," AIAA Journal, Vol. 11, No. 4, April 1973, pp. 444-451. Also see K. K. Kuo, R. Vichnevetsky and M. Summerfield, "Generation of an Accelerated Flame Front in a Porous Propellant," AIAA Paper 71-210.*

2. *C. W. Kitchens, Jr., "Flame Spreading in Small Arms Ball Propellant," BRL Report 1604, Ballistic Research Laboratories, August 1972.* (AD #750567)

3. *C. W. Kitchens, Jr., and N. J. Gerri, "Numerical and Experimental Investigation of Flame Spreading and Gas Flow in Gun Propellants," Proceedings of the 9th JANNAF Combustion Conference, Monterey, California, Vol. 1, September 1972. CPIA Publication No. 231, December 1972, pp. 115-125.*

parameters and critical assumptions in this model. These sensitivity studies were discussed at a JANNAF Workshop held at the BRL in November 1973. A review of this workshop, including a discussion of these sensitivity studies, is given in Reference 4.

## II. FLAME SPREADING MODEL

The theoretical model developed by Kuo et al[1] assumes that the charge loading density is sufficiently high so that the propellant bed can be treated as fixed; i.e., no propellant motion is allowed to take place in the bed. This model accounts for heat, mass and momentum exchange between the moving gas and the fixed propellant bed. The gas flow is governed by a system of hyperbolic partial differential equations based on one-dimensional time-dependent compressible flow. Empirical correlations are used to describe the heat and momentum losses in the gas. The position of the flame front in the propellant charge is predicted by the simultaneous solution of the gas flow through the porous charge and the transient heat conduction process occurring in an "average" propellant grain.

The equations[1] governing the gas flow through ball propellant are the continuity equation

$$\partial(\rho\phi)/\partial t + \partial(\rho\phi U)/\partial x = 6(1-\phi)\rho_p R/D \quad , \tag{1}$$

the momentum equation

$$\partial(\rho\phi U)/\partial t + \partial(\rho\phi U^2)/\partial x = g[-\phi\partial P/\partial x - 3(1-\phi)D_r/D] \quad , \tag{2}$$

and the energy equation

$$\phi\rho(\partial h/\partial t + U\partial h/\partial x) + \partial(\phi P)/\partial t + \phi U\partial P/\partial x =$$

$$[6(1-\phi)/D]\ [\rho_p R(h_f - h) + \rho_p RU^2/(2g) - \bar{h}_c(T-T_{ps}) + D_r U/2 \quad . \tag{3}$$

The density and temperature are assumed to be related to pressure by the ideal gas equation of state

$$P = \rho\bar{R}T \quad . \tag{4}$$

---

4. *H. Krier and W. F. Van Tassell, "A Review of the Workshop on Gas Dynamics Modeling of Reactive Flow Through Gun Propellant Charges," Proceedings of the 11th JANNAF Combustion Conference, Pasadena, California, Vol. 1, September 1974. CPIA Publication No. 261, December 1974, pp. 1-10.*

The drag and heat losses in the gas are described by empirical correlations for the drag force per one-half area of pellets, $D_r$, and the convective heat transfer coefficient, $\bar{h}_c$, in Eqs. (2) and (3). The gaseous mass addition due to propellant combustion is accounted for by the terms containing the propellant burning rate, R. The propellant grain distribution in the bed is described by the bed porosity, $\phi$. The porosity, sometimes called the void fraction, is the ratio of the pore volume to the spatial volume occupied by gas and/or propellant particles. By definition $o \leq \phi \leq 1$, with $\phi = 1$ corresponding to a volume element containing no propellant.

Eqs. (1) - (4) form a system of hyperbolic partial differential equations. The governing equations can be reduced to characteristic form and expressed as ordinary differential equations along the left- and right-running Mach lines and the particle path line. The compatibility equations are given in Reference 2 together with a method of characteristics procedure for obtaining numerical solutions. A computer program based on this procedure has been developed and used in the present sensitivity study. A preliminary version of this program was used in the calculations described in Reference 2. The present version of this program can account for a non-uniform initial porosity distribution in the bed and non-steady burning rate effects.

The flame spreading code has been used to predict flame spreading in the venting chamber configuration shown schematically in Figure 1. The chamber length and diameter, and the location of the pressure gauges in the chamber can be varied as input parameters. The right end of the chamber consists of a shear disk; the left end of the chamber contains the primer and primer vent tube. The chamber is filled with WC846 deterred double-base ball powder which is ignited by a FA-34 or FA-41 primer. A series of 5.56 and 7.62 mm diameter chambers similar to that shown in Figure 1 have been used to study flame spreading experimentally[5,6]. A transient compaction of the propellant charge occurs in the experiments immediately after primer initiation. This results in the propellant charge being pushed away from the primer vent tube by the initial primer blast. The transient propellant motion and the propellant bed compaction cannot be treated exactly in this model, because

---

5. *Private communication from Mr. W. H. Squire, Frankford Arsenal, February 1972.*

6. *N. J. Gerri, S. P. Pfaff and A. E. Ortega, "Gas Flow and Flame Spreading in Porous Beds of Ball Propellant," Proceedings of the 11th JANNAF Combustion Conference, Pasadena, California, Vol. 1, September 1974. CPIA Publication No. 261, December 1974, pp. 177-198.*

we assume the propellant bed is stationary. We do, however, assume that the propellant charge is initially set back a fixed distance from the primer, $x_p$, forming the primer blast compaction region shown in Figure 1. The length of the compaction region, $x_p$, and the initial porosity distribution $\phi(x)$ along the propellant bed can be specified as input parameters in the flame spreading code.

## III. COMPARISON WITH EXPERIMENTAL PRESSURE MEASUREMENTS IN VENTING CHAMBERS

The method of characteristics flame spreading code was originally developed to predict the pressure-time history and flame speed in a short venting chamber with a length of 3.81 cm. The results from this code, presented in Reference 2, were in substantial agreement with the finite-difference predictions of Kuo et al[1] and the experimental pressure measurements taken by Squire[5]. The agreement between the numerical predictions[1,2] and the experimental measurements[5] was encouraging in view of the many parameters which must be supplied as model inputs. Some uncertainty about the chamber length and gauge positions used in these comparisons created the need for another set of experiments. The experimental measurements conducted by Gerri et al[6] are used as the basis for determining the validity of the present calculations. The chamber length and gauge positions are now known with certainty, but many of the input parameters must be estimated using experimental data insufficient for the purpose; e.g., the drag correlation, the convective heat transfer correlation, the initial bed porosity distribution and the compaction distance.

In the present work the flame spreading code was used to predict the pressure-time history in 5.85 cm and 10.84 cm long venting chambers to determine if the fixed-bed model is still applicable as the chamber length increases. Gerri et al[6] have conducted an experimental study in 5.85 cm, 10.84 cm and 20.16 cm long venting chambers. They studied the effects of primer strength, primer vent hole geometry and the shear disk rupture pressure. All three of their chambers are similar to the 5.85 cm chamber depicted schematically in Figure 1. According to Reference 6 the experimental firings demonstrate the importance of two factors in long base-ignited propellant charges: (1) the "propellant-primer interface" and (2) the degree of initial compaction of the propellant bed by the primer blast. These two factors must be accounted for in the present fixed-bed model through input parameter specifications.

Gerri et al[6] have defined a "standard run" in their experimental firings because of the many parameters which were varied in their experiments. The standard run consists of: (1) a 7.62 mm diameter chamber 100% volumetrically loaded with WC846 deterred ball powder and ignited in a vertical orientation with the primer at the bottom; (2) a

stainless steel shear disk with a static burst pressure of 165 MPa; and (3) a FA-41 primer mounted in the standard 5.56 mm round vent configuration.

Numerical calculations were carried out to simulate the experimental standard run in the 5.85 cm and 10.84 cm chambers. The 5.85 cm long chamber is instrumented with three pressure gauges as shown in Figure 1; the 10.84 cm chamber has four gauges as described in Reference 6. The thermodynamic input parameters describing the properties of the gaseous combustion products and propellant were identical to those used in the calculations in Reference 2 for the 3.81 cm chamber. Nominal values were used for compaction distance, porosity distribution, and propellant burning rate; they are described in detail in Section IV.

Figure 2 shows a comparison of the calculations (C) and the experimental pressure measurements (E) for the 5.85 cm chamber. Comparisons are shown for all three pressure gauges used in this chamber. Gauge 1 is located at $x_1$ = 2.15 cm, with gauge 2 at $x_2$ = 3.42 cm and gauge 3 at $x_3$ = 4.69 cm. The distance x, shown in Figure 1, is measured from the end of the primer vent tube. The origin of time in Figure 2 is defined as the time that primer delivery begins (approximately 0.23 ms after the firing pin strikes the primer). The experimental records are terminated at 0.22 ms, the time that the peak pressure is recorded at gauge 3. We expect that shear disk rupture occurs approximately 0.02 ms before gauge 3 peaks. The numerical calculations are terminated at the time that the pressure on the shear disk reaches 110 MPa, the approximate time of shear disk rupture. The pressure level predicted at each gauge is in rough agreement with the experimental measurements at the time of shear disk rupture. The pressure-rise rate at each gauge and total time to shear disk rupture are in error. Shear disk rupture occurs at 0.60 ms in the calculations and at approximately 0.20 ms in the experiment. The predicted average flame spreading rate thus appears to be almost three times slower than is indicated in the experiment.

Similar calculations were carried out for the standard run in the 10.84 cm chamber. These calculations (C) are compared with the experimental measurements (E) in Figures 3a, b. Gauge 1 is located at $x_1$ = 3.38 cm, with the other three gauges at $x_2$ = 5.29 cm, $x_3$ = 7.20 cm and $x_4$ = 9.11 cm. The experimental records are terminated at 0.38 ms, the time that the peak pressure is recorded at gauge 4. Shear disk rupture occurs in this chamber approximately 0.02 ms before gauge 4 peaks. The numerical calculations are terminated at 1.55 ms when the pressure on the shear disk reaches 110 MPa. The pressures predicted at gauges 1, 2 and 3 are almost four times higher than the measured values at the time of shear disk rupture. The predicted peak pressure at gauge 4 is in error by 31%. The predicted pressure-rise rates at all four gauges are in general agreement with the experiment. The predicted total time to shear disk venting is more than three times the observed value.

This means that the predicted average flame spreading rate is more than three times too slow, similar to the slow flame spreading rate predicted in the 5.85 cm chamber.

The large differences between the predicted and experimental pressure levels may be caused by improper parameter input values. An appropriate adjustment of input values might yield better agreement with experiment. The large differences in shear disk rupture time, however, appear to be caused by a small flame spreading rate. This slow flame spreading rate could be caused by many factors in the fixed-bed model. These factors have each been analyzed separately in the sensitivity study in an attempt to determine which are most important.

## IV. PARAMETRIC SENSITIVITY STUDY

A parametric sensitivity study has been performed with the flame spreading code to study the importance of: (1) average particle size, (2) ignition criteria, (3) drag correlation, (4) convective heat transfer correlation, (5) compaction distance and bed porosity distribution, and (6) the burning rate equation. Most of the calculations were performed for the standard run in the 10.84 cm venting chamber. The goal of the parametric study was to find the most sensitive input parameters in the calculation and determine if some reasonable adjustment of parameter values would improve agreement with experiment; i.e., faster flame spreading through the bed and a reduced peak chamber pressure.

A total of 27 cases were computed for the 10.84 cm venting chamber with about half of these actually run to completion (shear disk rupture). A numerical calculation was performed in steps with intermediate-time results stored on magnetic tape so the calculation could be restarted. The results were examined as the calculation progressed and the calculation was terminated if desired. A completed case required about 10 minutes of computer time on the UNIVAC 1108, or 40 minutes on the BRLESC computer. The importance of each of the parameters studied will be described separately in terms of the calculations for the 10.84 cm chamber, unless otherwise stated.

### A. Average Particle Size

The present model[2] approximates the granular bed of WC846 propellant as a bed of spherical grains of uniform size. A visual examination of the propellant reveals that only the smallest particles are spherical. The larger particles resemble pancakes, due to the manufacturing process for rolled ball powder. The measured propellant particle size distribution used in the experimental firings[6] is shown in Table I. The particle size ranges from approximately 0.35 mm to more than 0.85 mm.

TABLE I. WC846 Particle Size Distribution Used in Experimental Firings[6]

| US Mesh No. | Size of Opening in Screen (mm) | % Total Weight |
|---|---|---|
| 20 | 0.84 | 0.89 |
| 25 | 0.71 | 6.92 |
| 30 | 0.59 | 35.18 |
| 35 | 0.50 | 32.89 |
| 40 | 0.42 | 21.97 |
| 45 | 0.35 | 2.15 |

For rounded particles approaching a spherical shape, the particle diameter of a narrow fraction (retained between adjacent screens with openings $d_a$ and $d_b$) can be obtained as the arithmetic mean $d_i = (d_a + d_b)/2$, or the geometric mean $d_i = (d_a d_b)^{\frac{1}{2}}$, of the dimensions of the screen openings. For a propellant sample with a wide range of particle sizes, such as the WC846 propellant in Table I, the method of averaging used to obtain a representative mean diameter can lead to different results and create uncertainty. Two methods for determining the mean diameter are discussed by Zabrodsky[7]. They are described by the equations

$$\frac{1}{d_A} = \frac{X_1}{d_1} + \frac{X_2}{d_2} + \cdots + \frac{X_n}{d_n} \quad , \tag{5}$$

$$d_B = X_1 d_1 + X_2 d_2 + \cdots + X_n d_n \quad ; \tag{6}$$

where $X_i$ is the weight fraction of a narrow fraction of diameter $d_i$. Eq. (6) generally yields larger values of the representative mean diameter than Eq. (5). The representative mean diameters obtained for the WC846 propellant, using the arithmetic mean method for a narrow fraction, are $d_A = 0.56$ mm and $d_B = 0.58$ mm. A nominal particle diameter of 0.53 mm was used in the standard run calculations shown in Figures 2 and 3. In general, for a fixed bed porosity $\phi$, increasing the nominal particle diameter decreases the bed resistance to gas flow, but also decreases the convective heat transfer rate. These two effects

7. *S. S. Zabrodsky, Hydrodynamics and Heat Transfer in Fluidized Beds, The M. I. T. Press, Cambridge, Massachusetts, 1966.*

compete with each other and the net result is not clear. The smaller bed resistance causes a larger gas velocity; the smaller convective heat transfer rate causes a slower propellant heating and hence slower propagation of the flame front through the propellant bed.

Sensitivity calculations were carried out using three nominal particle diameters: 0.53, 0.65 and 0.74 mm. The 0.74 mm case represents a 40% increase from the nominal diameter used in the standard run. No significant differences in the results were obtained. This implies that the value chosen for the mean particle diameter is not critical in the calculations.

## B. Ignition Criteria

The ignition model used in the calculation bases the onset of burning on the local propellant surface temperature, $T_{ps}$. The propellant surface temperature is determined by an integral solution of the heat conduction equation for an individual nominal diameter particle. Burning is assumed to start when the surface temperature reaches the ablation temperature, $T_a$. The burning rate is zero at this instant and it increases linearly with surface temperature until the ignition temperature, $T_i$, is reached, as described in Reference 2. The propellant burning rate is then given by $R = aP^n$ (when dynamic burning effects are neglected).

The standard run calculations used values of $T_a = 505°K$ and $T_i = 615°K$. In an attempt to increase the speed of the flame front, two cases were run with the assumed values of the ablation and ignition temperatures decreased. Case 1 used $T_a = 450°K$ and $T_i = 559°K$; a 9% decrease in $T_i$ from the standard value. Case 2 used $T_a = 394°K$ and $T_i = 504°K$, an 18% decrease in $T_i$ from the standard value, but much lower values than are experimentally justified. The results of these cases can be compared by looking at the calculated speed of the flame front as it passes gauge 2, almost midway down the chamber. The calculated flame speed in the standard run is 97 m/s. Case 1 gives a flame speed of 105 m/s, with case 2 predicting 113 m/s. Thus an 18% decrease in $T_i$ increases the flame speed at gauge 2 by 16%. This increased rate of flame spreading decreases the peak chamber pressure as expected, but only by 10% of the standard run value at the time the flame front passes gauge 2. This does not appear to be a significant difference in peak pressure in view of the much lower values observed experimentally.

C. Drag Correlation

Ergun's incompressible steady-state drag correlation[8] for flow through a fixed bed of spheres is used in the present calculations. The drag force acting on the gas per one-half area of pellets is described by

$$D_r = \frac{\rho U|U|}{3g\phi}\left[150\,\frac{(1-\phi)}{\phi}\left(\frac{\mu}{\rho UD}\right) + 1.75\right] . \qquad (7)$$

This correlation is valid for porosities over the range $0.4 \leq \phi \leq 0.7$ and for Reynolds numbers up to 3000, based on particle diameter. In the present venting chamber flow, the Reynolds number becomes much larger than this; on the order of $1\times10^6$. Another possible source of error in using the Ergun equation is that compressibility effects are neglected. Clearly, the Ergun correlation may improperly describe the drag in the venting chamber flow and may be in error by orders of magnitude. In general, particle roughness and particle shape should also be included in a more accurate correlation since they are known to be important in determining the pressure drop in packed beds.

In an effort to determine the sensitivity of the results to the drag correlation, the drag value given by the Ergun equation was arbitrarily reduced from the nominal value by 300% and 1000% in subsequent cases. The lower drag allows the flame front speed to increase and the predicted peak pressures are in closer agreement with the experimental values. The 300% decrease in drag from the nominal value causes a 34% increase in the flame front speed at gauge 2 and a 61% decrease in the peak chamber pressure at the time the flame front passes gauge 2. The 1000% decrease in drag causes the gas flow in the propellant bed to become supersonic shortly after primer initiation. The method of characteristics code was not programmed to treat the supersonic flow situation since the flow is normally subsonic. This case was thus terminated instead of adding the programming necessary to treat supersonic flow. These two cases show that the calculation is sensitive to the drag correlation and that a more appropriate drag correlation might improve the agreement with experiment.

D. Convective Heat Transfer Correlation

Denton's convective heat transfer correlation[9] for incompressible flow through a fixed porous bed was used in the standard run calculations.

---

8. *S. Ergun, "Fluid Flow Through Packed Columns," Chemical Engineering Progress, Vol. 48, No. 2, February 1952, pp. 89-94.*

9. *W. H. Denton, "The Heat Transfer and Flow Resistance for Fluid Flow through Randomly Packed Columns," Institution of Mechanical Engineers and American Society of Mechanical Engineers, London, 1951, p. 370. Also see E. R. G. Eckert and R. M. Drake, Heat and Mass Transfer, McGraw-Hill Book Co., Inc., 1959, p. 253.*

This correlation is valid for only one porosity ($\phi = 0.370$) and is thus invalid over most of the range of porosities encountered in the venting chamber, approximately $0.2 \leq \phi \leq 1$. Also, the correlation is only valid over the Reynolds number range $500 \leq Re \leq 5 \times 10^4$. Denton's correlation is described by the equation

$$Nu = 0.80\ (\phi Re)^{0.7}\ (Pr)^{0.33} \quad . \tag{8}$$

The Nusselt and Reynolds numbers are based on sphere diameter and in the standard run we assumed $Pr = 0.7$. The convective heat transfer coefficient, $\bar{h}_c$, required in Eq. (3), is calculated from Eq. (8) as

$$\bar{h}_c = k_g Nu/D = 0.80\ k_g\ (\rho |U| \phi/\mu)^{0.70}\ (Pr)^{0.33}\ (D)^{-0.30} \quad . \tag{9}$$

Eq. (9) was used to describe $\bar{h}_c$ in the standard run calculations, but, since a wider range of porosity values is required, a more general empirical formula is needed. An alternate correlation due to Timofeev[7]

$$Nu = \begin{cases} 0.106\ (Re) & 20 \leq Re \leq 200 \\ 0.61\ (Re)^{0.67} & Re > 2000 \end{cases}$$

has been incorporated into the code and tested. The Timofeev correlation generally gives larger values for the Nusselt number than the Denton correlation and hence a faster propellant heating and increased flame spreading rate. For the special case $\phi = 0.370$ it gives results for Nu that are approximately 13% larger than Denton's value at $Re = 1 \times 10^6$ and 25% larger at $Re = 5 \times 10^4$. The accuracy of the Timofeev correlation is "not very high" according to Reference 7 and hence a more accurate convective heat transfer correlation should be sought. It appears that an accurate heat transfer correlation is not presently available covering the parameter range of interest[10].

## E. Bed Porosity Distribution and Compaction Distance

In the present model the propellant bed is assumed to have a primer blast compaction region (free of propellant) adjacent to the primer vent tube. The compaction region results from the propellant charge being pushed away from the primer vent tube by the initial primer blast. The ensuing propellant motion results in packing the propellant bed causing the porosity of the bed to decrease from its original value at loading. The reduced bed length due to the primer blast packing has been verified

---

10. *H. Krier, W. Van Tassell, S. Rajan and J. T. VerShaw, "Model of Gun Propellant Flame Spreading and Combustion," BRL Contract Report 147, March 1974.* (AD #918842L)

experimentally[3,6] by firing a primer into a chamber loaded with an inert propellant simulant. The compaction distance, $x_p$, has been shown experimentally[6] to be roughly 2 cm in the 10.58 cm chamber. The standard run calculations assumed that the compaction distance was 0.95 cm and that the bed packing was uniform along the chamber, resulting in a uniform initial porosity $\phi = 0.30$. This initial uniform porosity distribution is illustrated in Figure 4. The assumption of uniform packing is not very realistic.

A more realistic assumption is that the primer blast causes tight packing of the bed adjacent to the primer and the remainder of the bed is only slightly disturbed. This effect was observed in the primer and inert propellant simulant tests[3], but could not be quantified. The capability of specifying a non-uniform initial porosity distribution in the bed was added to the code to test the sensitivity of the results to this latter assumption. The sensitivity calculations were performed with the initial porosity at the primer end varying between 0.09 and 0.38. The porosity was assumed to vary linearly with bed length. Figure 4 shows the porosity distribution assumed in the standard run together with two other cases considered in the sensitivity study. The distance $x$ is measured from the end of the primer vent tube. The initial porosity distribution, $\phi(x)$, and the compaction distance, $x_p$, must both be specified. The assumed values must conserve the total mass of propellant initially loaded into the chamber. Thus for a fixed charge weight, changing the value assumed for $x_p$ changes the initial porosity distribution $\phi(x)$. In case A, shown in Figure 4, the compaction distance, $x_p$, is held at same value used in the standard run, but the porosity is specified to vary linearly along the chamber length: $0.22 \leq \phi \leq 0.38$. In case B the compaction distance is increased to 2.0 cm, with $0.09 \leq \phi \leq 0.38$. In both cases A and B, $\phi = 1.0$ over the length $x_p$, reflecting the absence of propellant in the compaction region.

The numerical calculations for ten cases with various initial porosity distributions have shown that the compaction distance, $x_p$, and initial porosity distribution, $\phi(x)$, are very sensitive parameters. A case discussed at the end of this section will illustrate this sensitivity. The results for case A in Figure 4 predicted a 5% slower flame spreading rate than the standard run and an increase in the peak chamber pressure by 4%. The results for case B predicted a 22% slower flame spreading rate than the standard run and a 6% increase in the peak chamber pressure. Increasing the compaction distance, $x_p$, tends to decrease the flame spreading rate and, in general, the more tightly the bed is packed by the primer blast, the slower the flame spreading rate. The best agreement with the experimental values came from the uniform compaction assumption used in the standard run, but this agreement was not satisfactory as discussed previously.

A similar set of sensitivity calculations have been carried out for the standard run in the 5.85 cm long venting chamber. The experimental measurements show a peak chamber pressure of approximately 350 kPa at the time of shear disk rupture. The numerical predictions for the peak chamber pressure range from 280 to 690 kPa depending on the length assumed for the compaction distance (using a uniform bed porosity in each case). The lowest peak pressure results were obtained with the largest assumed compaction distance, $x_p$ = 0.5 cm. The highest peak pressure results were obtained with $x_p$ = 0 cm. Thus by varying $x_p$ from 0 to 0.5 cm the peak chamber pressure can be reduced from 690 to 280 kPa, a 59% reduction. The compaction distance appears to be an extremely sensitive parameter in the 5.85 cm chamber. The trend of peak pressure decreasing as $x_p$ is increased in the 5.85 cm chamber is different from that predicted in the 10.84 cm chamber.

F. Burning Rate Equation

The WC846 ball propellant is deterred during manufacture to give an almost neutral burning grain. It appears that the best approximation to the steady burning rate is obtained by assuming that one of two different expressions holds, depending on whether the highly deterred outer layers are burning or whether the undeterred inner core is burning. Calculations for the standard run used a single burning rate equation

$$R_s = 4.643 \times 10^{-2} \, p^{0.619} \qquad (10)$$

for simplicity. The two-equation burning rate model has been tested in the code. The inclusion of the deterred "slow" burning during the early-time, low pressure, part of flame spreading has a tendency to reduce the flame front speed. This increases the peak chamber pressure above that obtained in the standard run. It appears that dynamic burning effects may be important during this low pressure part of flame spreading because there is a very large positive pressure transient, $\partial P/\partial t > 0$, during the flame spreading interval. Positive pressure transients tend to accelerate the burning process and can lead to a much faster flame spreading rate than is predicted by steady burning analysis.

A non-steady burning rate equation discussed by Krier[11] has been added to the code to test the importance of dynamic burning effects. The steady burning rate, $R_s$ given by Eq. (10), is augmented by a dynamic burning term, to yield

---

11. *H. Krier, "Solid Propellant Burning Rate During a Pressure Transient," Comb. Sci. Tech., Vol. 5, 1972, pp. 69-73*

$$R_d = R_s \left[ 1 + \psi \left( \frac{n}{p} \frac{\alpha}{R_s^2} \right) \frac{\partial P}{\partial t} \right] \quad ; \qquad (11)$$

where n is the steady burning rate exponent, $\alpha$ is the thermal diffusivity of the propellant, and $\psi$ is a constant which can be determined by matching Eq. (11) to experimental values. Table II compares the burning rates predicted by the steady and dynamic burning rate equations, Eqs. (10) and (11), during the flame spreading period for the standard run in the 10.84 cm chamber using an assumed value of $\psi = 1.0$. The ratio $R_d/R_s$ is shown in Table II for two positions in the chamber at each time: (1) the position of the peak chamber pressure, and (2) the position of the flame front. We see from this table that the dynamic burning term is very important at early times (0.05 ms) while the pressure is relatively low. At the end of the flame spreading period (1.55 ms) the pressure level is very high and dynamic burning effects are negligible. The dynamic burning effect is most important at the flame front position because $\partial P/\partial t$ is largest there. The inclusion of the dynamic burning effect increases the flame front speed and lowers the peak chamber pressure, giving better agreement with experiment. Unfortunately, the dynamic burning equations that are presently available, such as Eq. (11), are only valid for weak pressure transients because they are based on small perturbation analyses. They are not really suitable for the flame spreading problem because large pressure transients are present. These equations cannot be employed quantitatively in such cases without using them beyond their range of validity. Table II shows that the dynamic burning rate is 45.5 times larger than the steady burning rate at 0.05 ms. We expect that a ratio of 45.5 is much higher than the actual physical ratio, but that the trend is correctly predicted and dynamic burning effects are important in this problem.

TABLE II. Value of $R_d/R_s$ During Flame Spreading for the Standard Run in 10.84 cm Chamber

| Time (ms) | Peak Pressure Position | Flame Front Position |
|---|---|---|
| 0.05 | 45.5 | 45.5 |
| 0.40 | 2.3 | 7.3 |
| 1.00 | 1.1 | 1.3 |
| 1.55 | ~1 | ~1 |

## V. CONCLUSIONS

Two important parameters have been identified in this study. The propellant bed compaction due to the primer blast (compaction distance) and the initial porosity distribution are both very important in determining the pressure-time history and the flame front speed in the present "fixed-bed" model. This packing information must be prescribed as initial conditions in the fixed-bed model. It appears that a two-phase flow model which can accurately account for propellant bed packing and fluidization is required for more realistic simulations.

Dynamic burning effects are probably significant during the early-time (low pressure) part of the flame spreading period. The steady burning rate equation $R_s = aP^n$ may be in error by an order of magnitude or more in the vicinity of the flame front. The inclusion of the dynamic burning effect accelerates the flame front and gives results which are in closer agreement with experiment. However, the adequacy of dynamic burning rate equations for sharp pressure transients must be determined experimentally.

Due to the many adjustable parameters in this problem, it is possible to make input adjustments to reproduce certain features of the experimental data, such as pressure-rise rates at certain chamber gauges. Gerri et al[6] show a comparison of their experimental data with one of the calculations obtained in this sensitivity study. The predicted pressure-rise rate, and maximum pressure at each gauge, is much closer to the experimental values than was shown in Figure 3 for our standard run. It appears, however, that the present fixed-bed model is not realistic enough to have predictive value for flame spreading in long chambers.

## VI. ADDENDUM

The author has recently learned of a drag correlation proposed by Kuo[12], based on new experiments for flow through porous beds. The Kuo correlation is based on data taken for flow at higher Reynolds numbers than Ergun's experiments and thus should be more appropriate for use in flame spreading predictions. The new correlation gives a value for the drag which is approximately one-third of the value indicated by the Ergun correlation, Eq. (7). The use of this new correlation in the present calculations would tend to increase the predicted flame spreading rate and reduce the peak chamber pressure.

---

12. *Private communication from Prof. K. K. Kuo, Department of Mechanical Engineering, Pennsylvania State University, September 1975.*

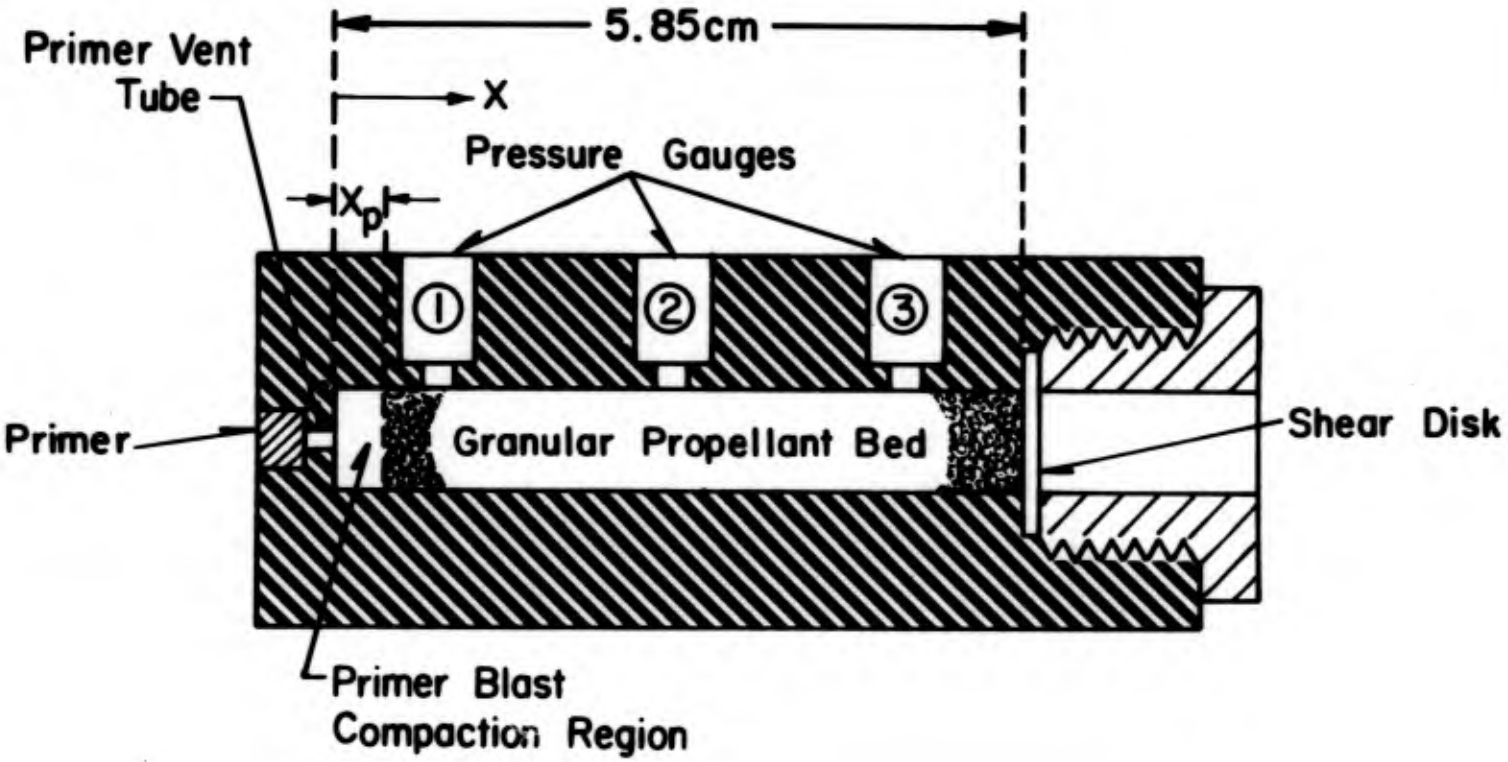


Figure 1. Schematic of Venting Chamber Used in Experimental Firings

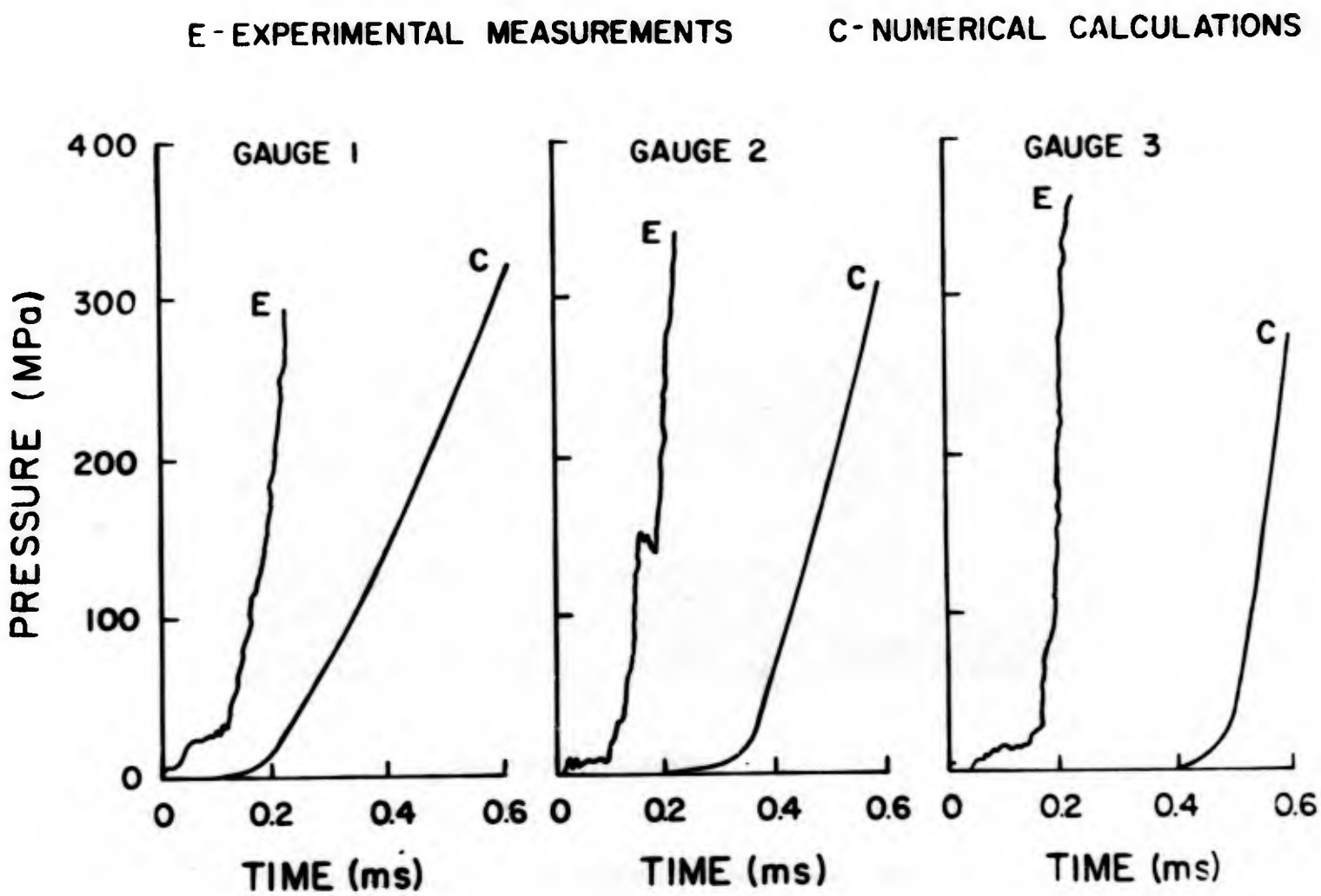


Figure 2. Comparison of Pressure-Time Predictions with Experimental Measurements for Standard Run in 5.85 cm Chamber

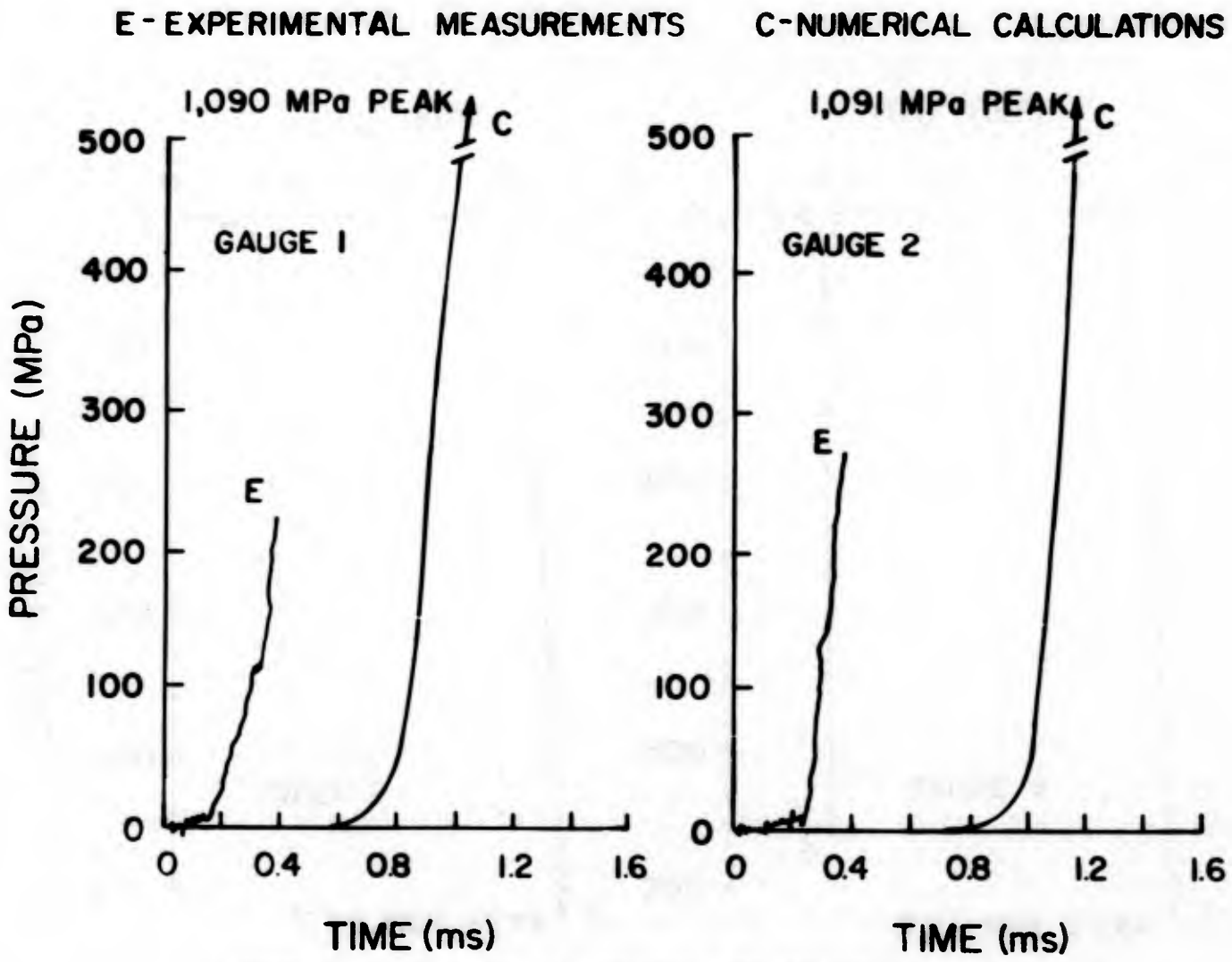


Figure 3a. Comparison of Pressure-Time Predictions at Gauges 1 and 2 with Experimental Measurements for Standard Run in 10.84 cm Chamber

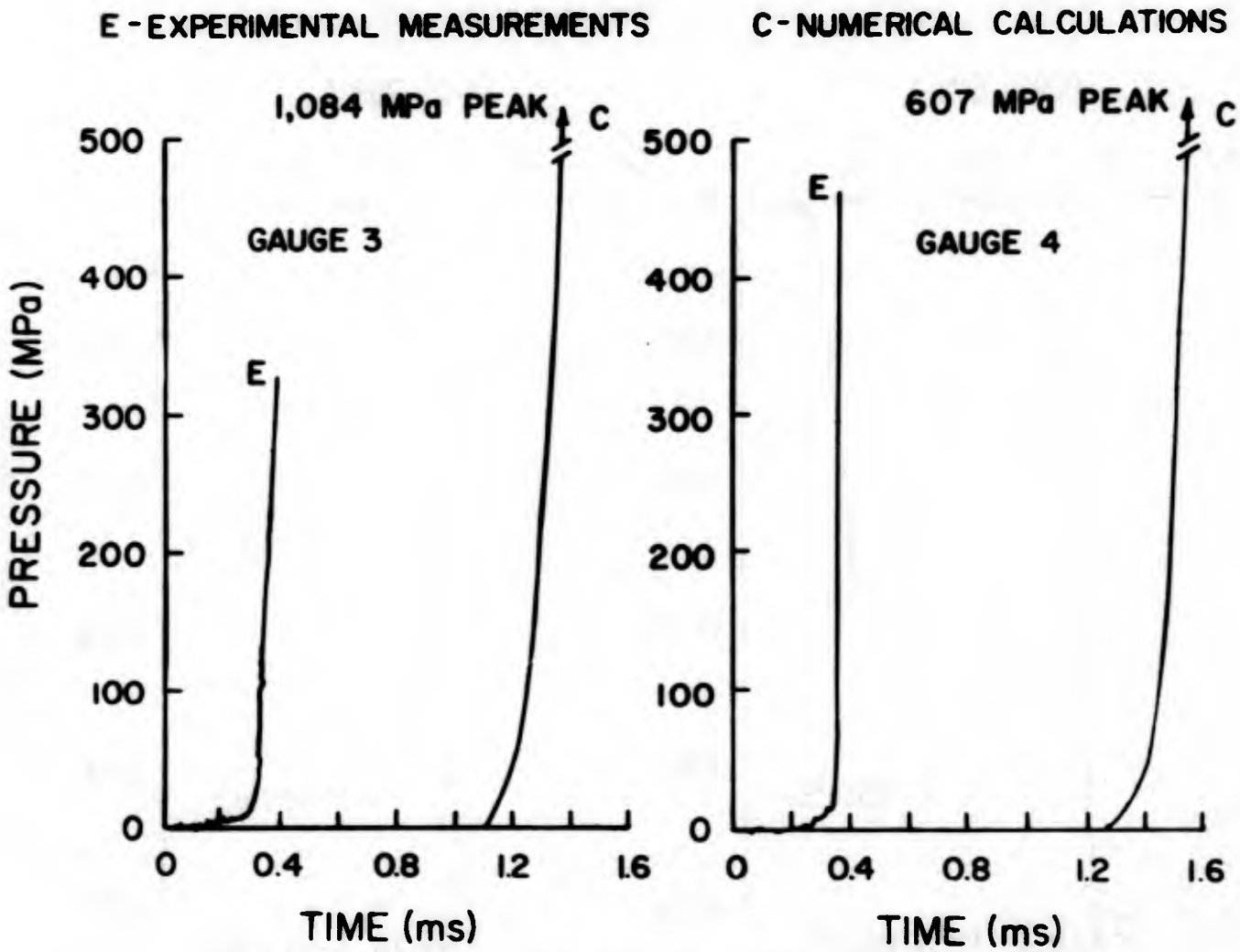


Figure 3b. Comparison of Pressure-Time Predictions at Gauges 3 and 4 with Experimental Measurements for Standard Run in 10.84 cm Chamber

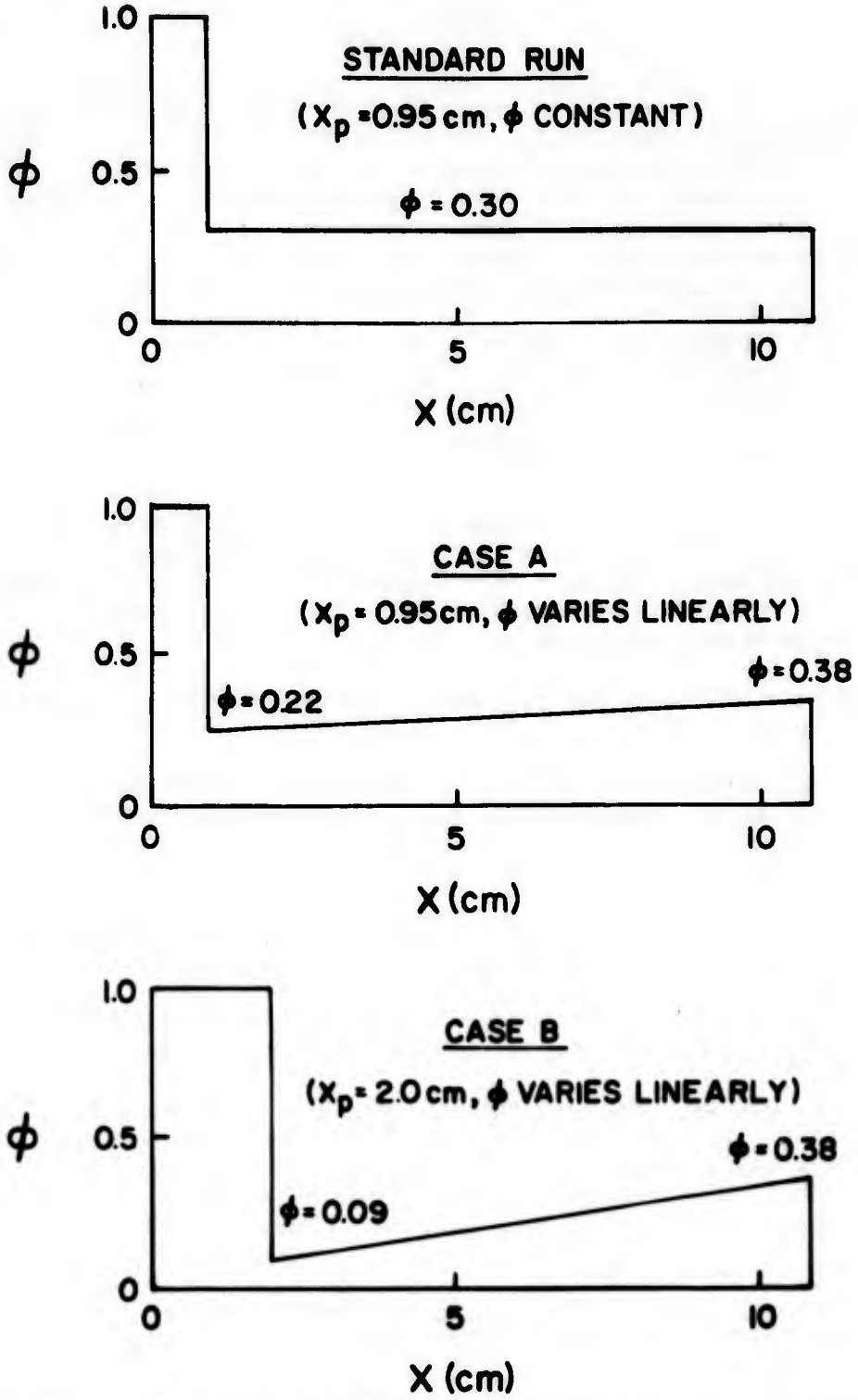


Figure 4. Comparison of Standard Run Initial Porosity Distribution and Two Alternate Distributions Assumed for 10.84 cm Chamber

## REFERENCES


1. K. K. Kuo, R. Vichnevetsky and M. Summerfield, "Theory of Flame Front Propagation in Porous Propellant Charges Under Confinement," AIAA Journal, Vol. 11, No. 4, April 1973, pp. 444-451. Also see K. K. Kuo, R. Vichnevetsky and M. Summerfield, "Generation of an Accelerated Flame Front in a Porous Propellant," AIAA Paper 71-210.

2. C. W. Kitchens, Jr., "Flame Spreading in Small Arms Ball Propellant," BRL Report 1604, Ballistic Research Laboratories, August 1972. (AD #750567)

3. C. W. Kitchens, Jr., and N. J. Gerri, "Numerical and Experimental Investigation of Flame Spreading and Gas Flow in Gun Propellants," Proceedings of the 9th JANNAF Combustion Conference, Monterey, California, Vol. 1, September 1972. CPIA Publication No. 231, December 1972, pp. 115-125.

4. H. Krier and W. F. Van Tassell, "A Review of the Workshop on Gas Dynamics Modeling of Reactive Flow Though Gun Propellant Charges," Proceedings of the 11th JANNAF Combustion Conference, Pasadena, California, Vol. 1, September 1974. CPIA Publication No. 261, December 1974, pp. 1-10.

5. Private communication from Mr. W. H. Squire, Frankford Arsenal, February 1972.

6. N. J. Gerri, S. P. Pfaff and A. E. Ortega, "Gas Flow and Flame Spreading in Porous Beds of Ball Propellant," Proceedings of the 11th JANNAF Combustion Conference, Pasadena, California, Vol. 1, September 1974. CPIA Publication No. 261, December 1974, pp. 177-198.

7. S. S. Zabrodsky, Hydrodynamics and Heat Transfer in Fluidized Beds, The M.I.T. Press, Cambridge, Massachusetts, 1966.

8. S. Ergun, "Fluid Flow Through Packed Columns," Chemical Engineering Progress, Vol. 48, No. 2, February 1952, pp. 89-94.

9. W. H. Denton, "The Heat Transfer and Flow Resistance for Fluid Flow Through Randomly Packed Columns," Institution of Mechanical Engineers and American Society of Mechanical Engineers, London, 1951, p. 370. Also see E. R. G. Eckert and R. M. Drake, Heat and Mass Transfer, McGraw-Hill Book Co., Inc., 1959, p. 253.

10. H. Krier, W. Van Tassell, S. Rajan and J. T. Ver Shaw, "Model of Gun Propellant Flame Spreading and Combustion," BRL Contract Report 147, March 1974. (AD #918842L)

11. H. Krier, "Solid Propellant Burning Rate During a Pressure Transient," Comb. Sci. Tech., Vol. 5, 1972, pp. 69-73.

12. Private communication from Prof. K. K. Kuo, Department of Mechanical Engineering, Pennsylvania State University, September 1975.

## LIST OF SYMBOLS

| | |
|---|---|
| $a$ | burning rate coefficient, m/s |
| $c_p$ | powder gas specific heat at constant pressure, N-m/kg-°K |
| $d_a$, $d_b$ | dimensions of openings of adjacent screens, m |
| $d_i$ | particle diameter of narrow fraction of screened ball propellant, m |
| $d_A$, $d_B$ | representative mean diameter of ball propellant, m |
| $g$ | conversion constant, $m/s^2$ |
| $h$ | enthalpy per unit mass, N-m/kg |
| $h_f$ | enthalpy per unit mass at propellant flame temperature, N-m/kg |
| $\bar{h}_c$ | average convective heat transfer coefficient, N/m-s-°k |
| $k_g$ | thermal conductivity of powder gas, N/s-°K |
| $t$ | time, s |
| $x$ | axial coordinate measured from end of primer vent tube, m |
| $x_i$ | pressure gauge locations in venting chamber, m |
| $x_p$ | length of primer blast compaction region, m |
| $D$ | instantaneous mean diameter of ball propellant, m |
| $D_r$ | drag force per half pellet area, $N/m^2$ |
| Nu | Nusselt number ($= \bar{h}_c D/k_g$), nondimensional |
| P | pressure, Pa (MPa = $1 \times 10^6$ $N/m^2$ ~ 9.87 atm.) |
| Pr | Prandtl number ($= \mu c_p/k_g$), nondimensional |
| $R$ | propellant burning rate, m/s |
| $\bar{R}$ | gas constant, N-m/kg-°K |

| | |
|---|---|
| Re | Reynolds number (= $\rho UD/\mu$), nondimensional |
| T | powder gas temperature, °K |
| $T_a$ | propellant ablation temperature, °K |
| $T_i$ | propellant ignition temperature, °K |
| $T_{ps}$ | instantaneous propellant surface temperature, °K |
| U | powder gas velocity, m/s |
| $X_i$ | weight fraction of narrow fraction with diameter $d_i$, nondimensional |
| $\alpha$ | propellant thermal diffusivity, $m^2/s$ |
| $\mu$ | powder gas absolute viscosity, kg/m-s |
| $\rho$ | powder gas density, $kg/m^3$ |
| $\rho_p$ | propellant density, $kg/m^3$ |
| $\phi$ | porosity or void fraction, nondimensional |
| $\psi$ | constant in dynamic burning equation, Eq. (11), nondimensional |

Subscripts

| | |
|---|---|
| d | dynamic burning rate, Eq. (11) |
| s | steady burning rate, Eq. (10) |

DISTRIBUTION LIST

| No. of Copies | Organization |
|---|---|
| 12 | Commander<br>Defense Documentation Center<br>ATTN: DDC-TCA<br>Cameron Station<br>Alexandria, VA 22314 |
| 1 | Commander<br>US Army Materiel Command<br>ATTN: AMCDMA-ST<br>5001 Eisenhower Avenue<br>Alexandria, VA 22333 |
| 1 | Commander<br>US Army Materiel Command<br>ATTN: AMCRD-T<br>5001 Eisenhower Avenue<br>Alexandria, VA 22333 |
| 1 | Commander<br>US Army Materiel Command<br>ATTN: AMCRD-R<br>5001 Eisenhower Avenue<br>Alexandria, VA 22333 |
| 1 | Commander<br>US Army Aviation Systems Command<br>ATTN: AMSAV-E<br>12th and Spruce Streets<br>St. Louis, MO 63166 |
| 1 | Director<br>US Army Air Mobility Research and Development Laboratory<br>Ames Research Center<br>Moffett Field, CA 94035 |
| 1 | Commander<br>US Army Electronics Command<br>ATTN: AMSEL-RD<br>Fort Monmouth, NJ 07703 |
| 1 | Commander<br>US Army Missile Command<br>ATTN: AMSMI-R<br>Redstone Arsenal, AL 35809 |
| 1 | Commander<br>US Army Tank Automotive Command<br>ATTN: AMSTA-RHFL<br>Warren, MI 48090 |
| 2 | Commander<br>US Army Mobility Equipment Research & Development Center<br>ATTN: Tech Docu Cen, Bldg. 315<br>AMSME-RZT<br>Fort Belvoir, VA 22060 |
| 1 | Commander<br>US Army Armament Command<br>Rock Island, IL 61202 |
| 2 | Commander<br>US Army Frankford Arsenal<br>ATTN: Mr. Ludwig Stiefel<br>Mr. Sidney Goldstein<br>Philadelphia, PA 19137 |
| 3 | Commander<br>US Army Picatinny Arsenal<br>ATTN: Mr. Fred Fitzsimmons<br>Mr. Charles Lenchitz<br>Mr. A. A. Loeb<br>Dover, NJ 07801 |
| 1 | Commander<br>US Army Harry Diamond Labs<br>ATTN: AMXDO-TI<br>2800 Powder Mill Road<br>Adelphi, MD 20783 |
| 1 | Director<br>US Army TRADOC Systems Analysis Activity<br>ATTN: ATAA-SA<br>White Sands Missile Range<br>New Mexico 88002 |
| 1 | Commander<br>US Army Research Office<br>ATTN: Dr. R. E. Singleton<br>P. O. Box 12211<br>Research Triangle Park, NC 27709 |

DISTRIBUTION LIST

| No. of Copies | Organization |
|---|---|
| 1 | Commander<br>US Army Waterways Experiment Station<br>ATTN: Mr. R. H. Malter<br>Vicksburg, MS 39180 |
| 3 | Commander<br>US Naval Air Systems Command<br>ATTN: AIR-604<br>Washington, DC 20360 |
| 4 | Commander<br>US Naval Ordnance Station<br>ATTN: Mr. A. Horst<br>Mr. W. Burnett<br>Dr. C. Dale<br>Tech Lib<br>Indian Head, MD 20640 |
| 2 | Commander<br>David W. Taylor Naval Ship Research & Development Center<br>ATTN: Dr. H. J. Lugt, Code 1802<br>Tech Library<br>Bethesda, MD 20084 |
| 2 | Commander<br>US Naval Surface Weapons Center<br>ATTN: Dr. M. Ciment<br>Mathematics Dept<br>Dr. R. Bernecker<br>Code 231<br>Silver Spring, MD 20910 |
| 4 | Commander<br>US Naval Surface Weapons Center<br>ATTN: Code GBC, Mr. J.L. East<br>Mr. Tschirn<br>Code GR, Mr. W.G. Soper<br>Technical Library<br>Dahlgren, VA 22448 |
| 1 | AFATL (DLY)<br>Eglin AFB, FL 32542 |
| 1 | AFATL (DLDG)<br>Eglin AFB, FL 32542 |
| 1 | AFATL (DLRV)<br>Eglin AFB, FL 32542 |
| 1 | Director<br>National Aeronautics and Space Administration<br>Ames Research Center<br>ATTN: Tech Lib<br>Moffett Field, CA 94035 |
| 1 | Director<br>National Aeronautics and Space Administration<br>Langley Research Center<br>ATTN: Tech Lib<br>Langley Station<br>Hampton, VA 23365 |
| 1 | Director<br>National Aeronautics and Space Administration<br>Lewis Research Center<br>ATTN: MS 60-3, Tech Lib<br>21000 Brookpark Road<br>Cleveland, OH 44135 |
| 1 | Director<br>Jet Propulsion Laboratory<br>ATTN: Tech Lib<br>4800 Oak Grove Drive<br>Pasadena, CA 91103 |
| 1 | ARO, Inc.<br>ATTN: Tech Lib<br>Arnold AFS, TN 37389 |
| 1 | Brunswick Corporation<br>ATTN: Mr. B. N. Firebaugh<br>Route 1, Box 300<br>Sugar Grove, VA 24375 |

DISTRIBUTION LIST

| No. of Copies | Organization |
|---|---|
| 1 | Calspan Corporation<br>ATTN: Mr. Ed Fischer<br>4455 Genesee Street<br>Buffalo, NY 14221 |
| 2 | Hercules Inc.<br>ATTN: Dr. Lee Baxter<br>Dr. M. W. Beckstead<br>Magna, UT 84044 |
| 1 | Sandia Laboratories<br>ATTN: Tech Lib<br>P. O. Box 5800<br>Albuquerque, NM 87115 |
| 1 | United Aircraft Corporation<br>Research Laboratories<br>ATTN: Library<br>East Hartford, CT 06108 |
| 1 | California Institute of Technology<br>Guggenheim Aeronautical Lab<br>ATTN: Tech Library<br>Pasadena, CA 91104 |
| 1 | Cornell University<br>Graduate School of Aero Engr<br>ATTN: Library<br>Ithaca, NY 14850 |
| 1 | Georgia Institute of Tech<br>School of Aerospace Engineer<br>ATTN: Prof. Ben T. Zinn<br>Atlanta, GA 30332 |
| 1 | The Johns Hopkins University<br>ATTN: Tech Lib<br>Baltimore, MD 21218 |
| 1 | Massachusetts Inst of Technology<br>ATTN: Tech Library<br>77 Massachusetts Avenue<br>Cambridge, MA 02139 |
| 1 | Pennsylvania State University<br>Dept of Mechanical Engineering<br>ATTN: Prof. Kenneth K. Kuo<br>University Park, PA 16802 |
| 2 | Princeton University<br>Guggenheim Laboratories<br>ATTN: Dr. Leonard H. Caveny<br>Prof M. Summerfield<br>Princeton, NJ 08540 |
| 1 | Southwest Research Institute<br>Applied Mechanics Reviews<br>8500 Culebra Road<br>San Antonio, TX 78228 |
| 1 | University of Illinois<br>Aeronautical and Astronautical Engineering Department<br>ATTN: Prof. Herman Krier<br>105 Transportation Building<br>Urbana, IL 61801 |
| | Aberdeen Proving Ground |
| | Marine Corps Ln Ofc<br>Dir, USAMSAA |